# Diffractive production of pions by neutrinos

Marat Siddikov

(In collaboration with B. Kopeliovich, Iván Schmidt)

UNIVERSIDAD TECNICA
FEDERICO SANTA MARIA

Williamsburg, Virginia, USA
July 27, 2012

(PRD 84 (2011), 033012, PRC 84 (2011), 024608, PRD 85 (2012), 073003)

# Kinematics

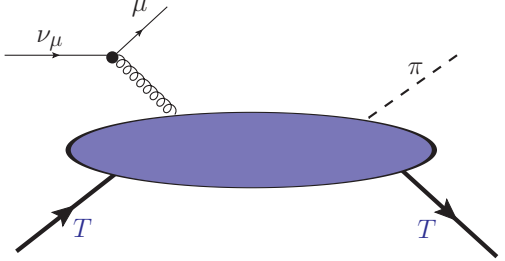


- Diffractive pion production,
  - CC: $\nu\, T \longrightarrow l\, \pi^+\, T$
  - NC: $\nu\, T \longrightarrow \nu\, \pi^0\, T$
  - also applies to other goldstones $(K, \eta)$

$$E_\nu = \frac{p\cdot k_\nu}{m_N}, \nu = \frac{p\cdot q_W}{M}, y = \frac{p\cdot q_W}{p\cdot k}$$

- (Minerva@Fermilab, 2011)

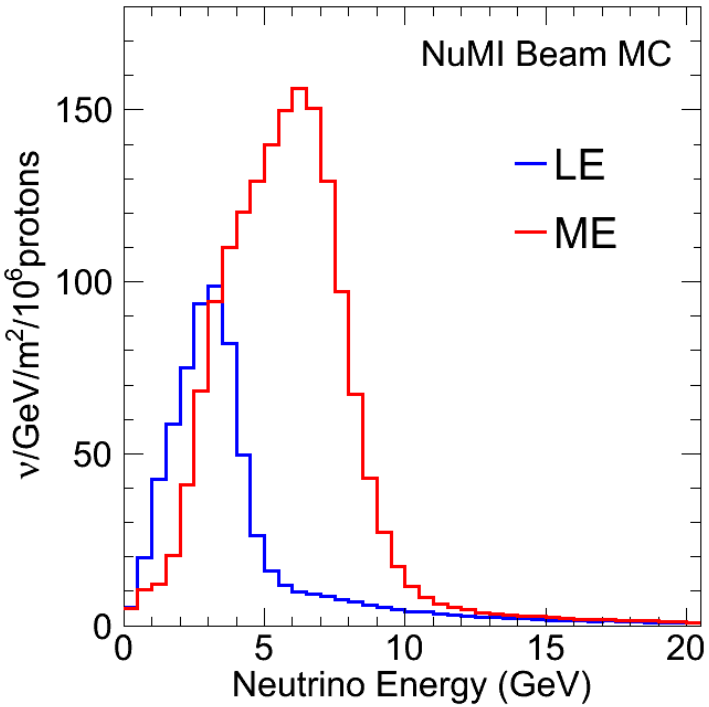


$$Q^2 = -q_W^2 = 4E_\nu(E_\nu - \nu)\sin^2\frac{\theta}{2} + \mathcal{O}\left(m_l^2\right)$$

$$t = (p' - p)^2 = \Delta^2 = t_{min} - \Delta_\perp^2$$

- ★ High statistics, *differential* x-sections are measured
- ★ Different targets ($H_2O$, He, C, CH, Fe, Pb)

# Why goldstone production ?

- Background in $\nu_\mu \to \nu_e$ (misidentification of $\pi_0$, $\pi_0 \to 2\gamma$)

  (MiniBooNE [PLB 664, 41 (2008)], SciBooNE [PRD 81, 111102 (2010)])

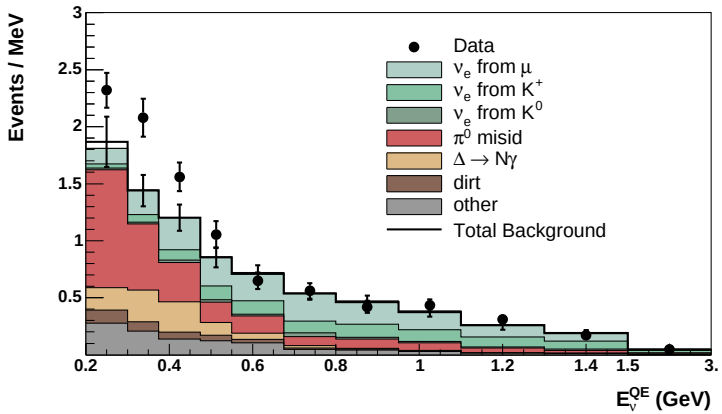


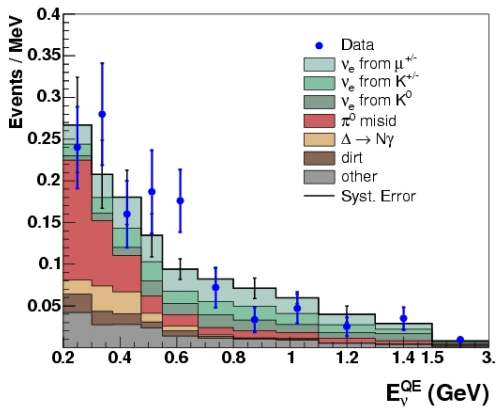


  (MiniBooNE [PRL 102, 101802 (2009); arXiv:1201.1519] )

- Backgrounds in rare processes:

  Atmospheric $\nu$ + material of detectors $\longrightarrow$ extra $\pi, K, \eta$

  - Planned LAGUNA experiment (proton decay studies):
    - ★ Grand Unified Models: $p \to e^+\pi_0$, $T \sim 10^{36} y$
    - ★ SUSY: $p \to K^+\bar{\nu}$, $T \sim 10^{34} y$

    (Current experimental limit: $T \gtrsim 5 \times 10^{33} y$ (SuperKamiokande: PRL 83(1999), 1529; PRL 83(1999), 1529; Int. J. Mod. Phys. A 16S1B (2001) 855.))

# Goldstones as probes of GPD flavour structure

Bjorken regime ($Q^2 \to \infty, x_B = Q^2/2m_N\nu = const$)

- (Collins, *et. al.*, PRD 56 (1997), 2982): factorization for longitudinal, suppression by $1/Q^2$ for transverse

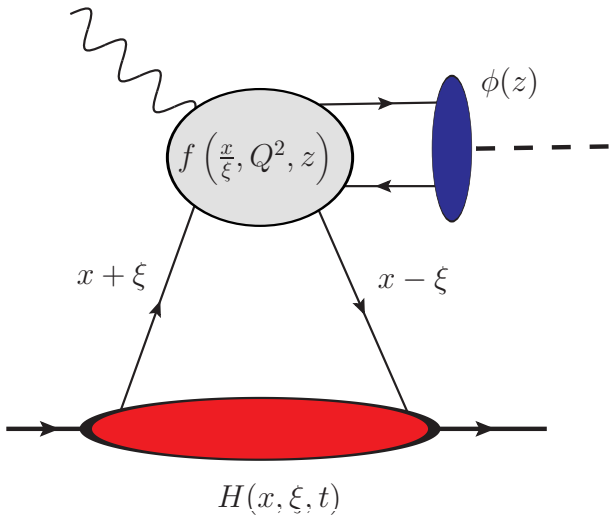


$$\mathscr{M} = \int dx\, dz\, f_{ij}\left(\frac{x}{\xi}, Q^2, z\right) \times H_i(x,\xi,t)\phi_j(z)$$

(ep)DVMP: LO hard part $f\left(\frac{x}{\xi}, Q^2, z\right)$ – (Vanderhaeghen *et. al.*, PRL **80** (1998) 5064)

$$\mathscr{M} \propto \frac{\alpha_s}{Q}\int dz\, \frac{\phi(z)}{z}\left(\mathscr{A}\,\bar{N}\gamma_+\gamma_5 N + \mathscr{B}\,\bar{N}\frac{i\sigma^{+k}\Delta_k}{2m}N\right),$$

$$\mathscr{A}, \mathscr{B} = \int dx\, H_M(x,\xi)C_M(x,\xi)$$

# Current knowledge of GPDs (from $ep$ @HERA and @JLAB)

- For each flavour and for gluon there are 8 GPDs:

$$\begin{aligned} \bar{\psi}\gamma_+\psi &\rightarrow (H, E) \\ \bar{\psi}\gamma_+\gamma_5\psi &\rightarrow (\tilde{H}, \tilde{E}) \\ \bar{\psi}\sigma_{+\perp}\psi &\rightarrow (H_T, E_T, \tilde{H}_T, \tilde{E}_T) \end{aligned}$$

- DVCS: the cleanest probe, but flavour structure unknown, $H(x,\xi,t) = \sum_f e_f^2 H^f(x,\xi,t)$
- wDVCS: $H(x,\xi,t) = \sum_f e_f g_w^f H^f(x,\xi,t)$ (Monday talk by W. Melnitchouk)
- DVMP: for vector mesons $\phi_\rho(z)$ unknown (even if $\phi_\rho(z)\big|_{endp.} = 0$); for pion $\phi(z) \approx 6z(1-z)$, but in $ep$ only sensitive to $\tilde{H}, \tilde{E}$:

$$\mathscr{A}_{\pi_0 p} \sim \int dx \left( \frac{1}{x-\xi+i0} + \frac{1}{x+\xi-i0} \right) \left( e_u \tilde{H}_u(x,\xi) - e_d \tilde{H}_d(x,\xi) \right)$$

$$\mathscr{A}_{\pi_+ n} \sim \int dx \left( \frac{e_u}{x-\xi+i0} + \frac{e_d}{x+\xi-i0} \right) \left( \tilde{H}_u(x,\xi) - \tilde{H}_d(x,\xi) \right)$$

To get $\mathscr{B}$ replace $\tilde{H} \rightarrow \tilde{E}$

# GPDs from $\nu p \to \pi p$ ???

- Vector channel is the same as in $ep$, in axial–sensitivity to $(H, E)$ [and gluons].
- Goldstone DAs are close to $\phi(z) \approx 6z(1-z)$ (parametricaly $\mathcal{O}(m_q/\Lambda)$, numerically deviations 10-20%).
- Heavy boson channel: The same 4 diagrams as for photons

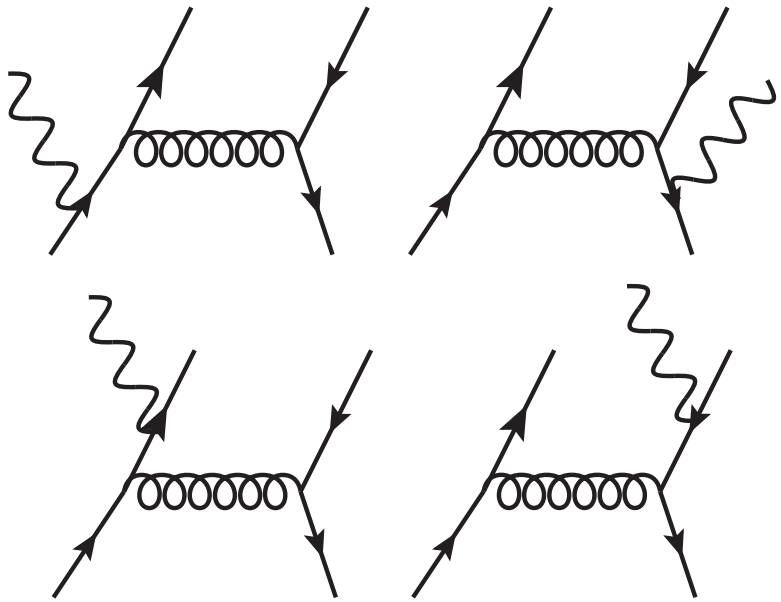

# GPDs from $\nu p \to \pi p$ ???

- Vector channel is the same as in $ep$, in axial–sensitivity to $(H, E)$ [and gluons].
- Goldstone DAs are close to $\phi(z) \approx 6z(1-z)$ (parametricaly $\mathscr{O}(m_q/\Lambda)$, numerically deviations 10-20%).
- Heavy boson channel:

$$\mathscr{A}_{\pi_0 p} \sim \int dx\, C_+(x,\xi)\,(H_u(x,\xi) + H_d(x,\xi)) + \mathscr{A}_g$$

$$\mathscr{A}_{\pi_+ n} \sim \int dx\, C_{ud}(x,\xi)\,(H_u(x,\xi) - H_d(x,\xi))$$

$$\mathscr{A}_{K_+ p} \sim \int dx\, C_+(x,\xi)\,(H_u(x,\xi) + H_s(x,\xi)) + \mathscr{A}_g$$

$$\mathscr{A}_{\eta p} \sim \int dx\, C_+(x,\xi)\,(H_u(x,\xi) - H_d(x,\xi) + 2H_s(x,\xi)) + \mathscr{A}_g$$

(.....)

(in preparation)

To get $\mathscr{B}$, replace $H \to E$. $\mathscr{A}_g \sim C(x,\xi) \otimes H^g$

At $x \gtrsim 0.1$ gluons are negligible, at $x \ll 1$ gluons dominate, we'll discuss them later

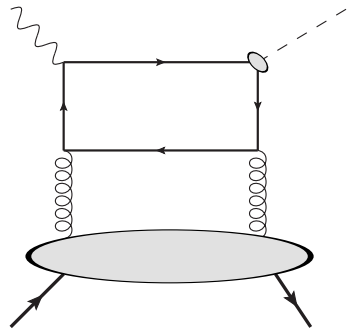

# Estimate for $\nu p \to \pi p$ with GPD models

(simple DD, no $D$-term, no $\tilde{H}(x,\xi,t), \tilde{E}(x,\xi,t), E(x,\xi,t)$)

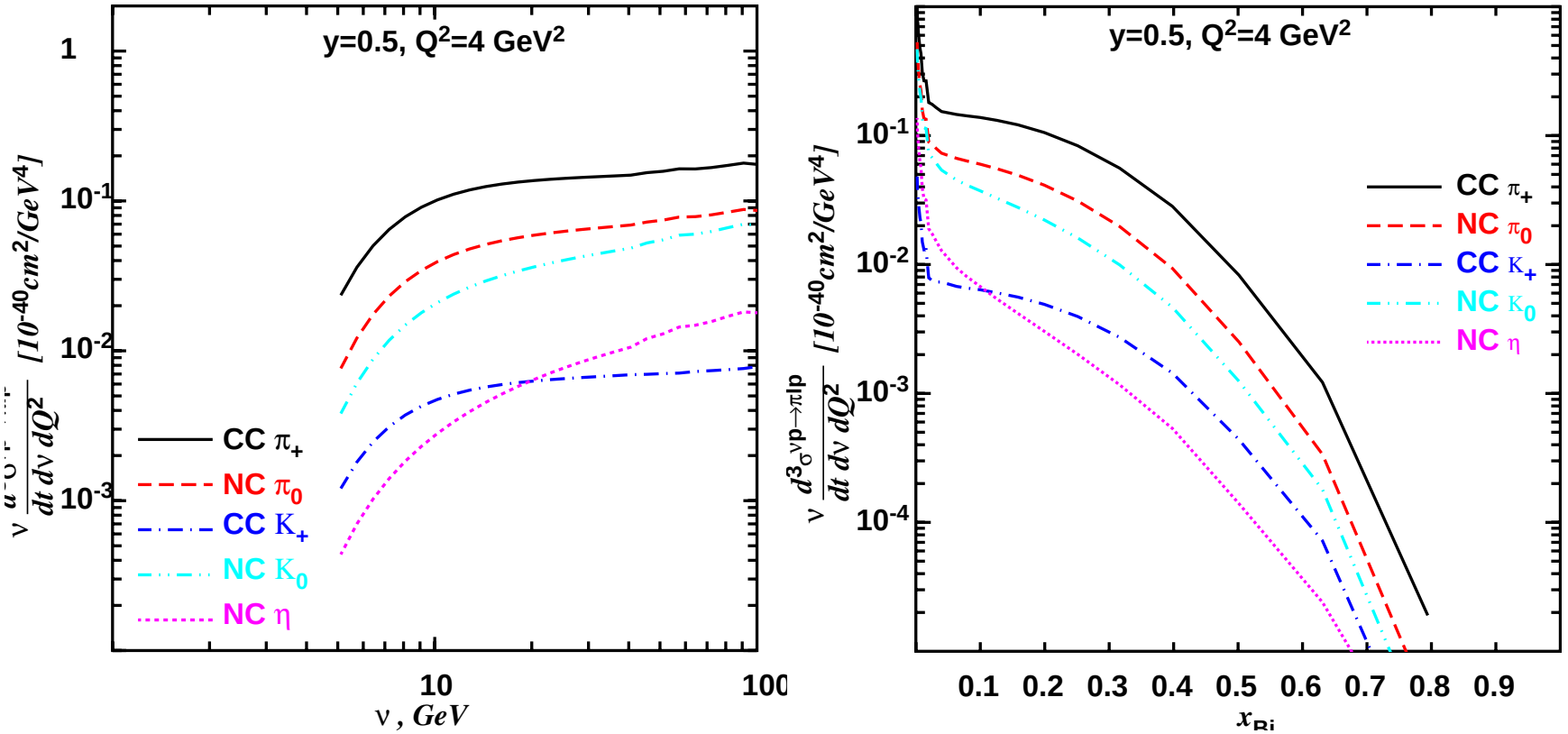


Figure: Cross-section $\nu d\sigma/dtd\nu dQ^2$ with DD model of GPD $H$

- CC $K_+$-production is Cabibbo-suppressed
- NC $\eta$-production is mostly sensitive to strange quarks

# Estimate for $\nu p \to \pi p$ with GPD models

(Kroll-Goloskokov model (EPJC 59 (2009) 809 ) [DD for $H(x,\xi,t), E(x,\xi,t)$])

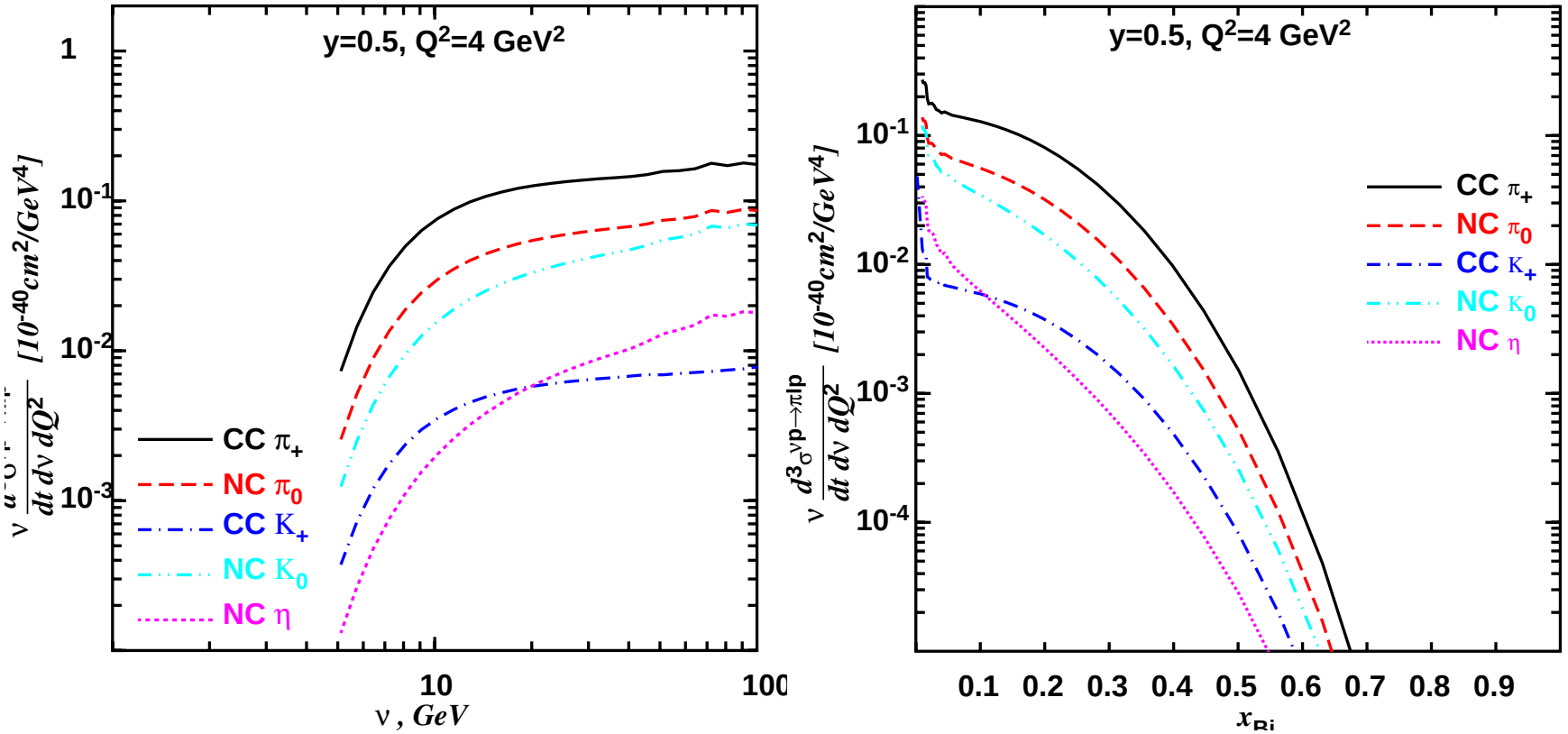


Figure: Cross-section $\nu d\sigma/dtd\nu dQ^2$ with Kroll-Goloskokov model

- $\nu d\sigma/dtd\nu dQ^2 \sim (1-\xi^2)\,|\mathscr{H}|^2 - \mathscr{O}(\xi^2)\,|\mathscr{E}|^2 - \mathscr{O}(\xi)\,(\mathscr{H}\mathscr{E}^* + \mathscr{E}\mathscr{H}^*)$

- Single-goldstone production in Bjorken kinematics could complement measurements of GPDs in $ep$ and reveal their flavour structure.

Unfortunately, this regime is not studied up to now, all the differential cross-sections are for low-energies (and low virtualities $Q^2$).

# PCAC-based models: Adler relation

$$\left.\frac{d\sigma_{\nu T\to lF}}{d\nu dQ^2}\right|_{Q^2=0} = \frac{G_F^2}{2\pi} f_\pi^2 \frac{E_\nu - \nu}{E_\nu \nu} \sigma_{\pi T\to F}$$

- In real measurements $q^2 \neq 0$, so AR requires extrapolation.

AR $\neq$ Pion dominance:

$$T_\mu(...) \sim \frac{q_\mu}{q^2 - m_\pi^2} + T_\mu^{non-pion}(...),$$

but lepton currents are conserved, so

$$q_\mu L_{\mu\nu} = \mathscr{O}(m_l)$$

$\Rightarrow$AR survives due to heavier hadrons and $\chi$-sym.

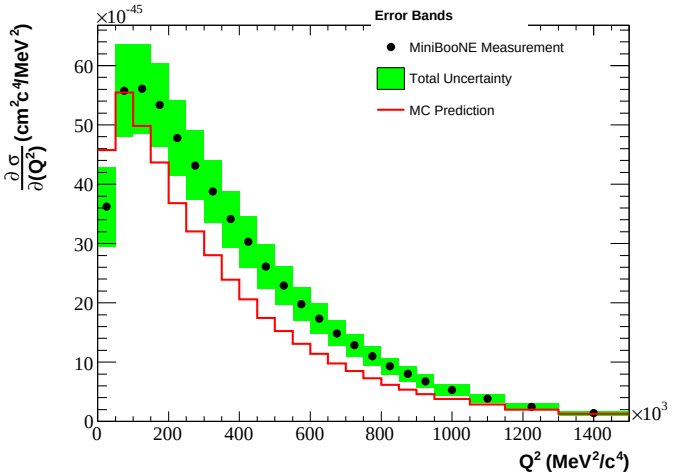


(MiniBooNE, PRD 83(2010), 052007)

- $\sigma \sim (1 + Q^2/m_A^2)^{-2}$, $m_A \sim 1$ GeV
- Contributions from transverse part and from the vector part ($\mathscr{O}(q^2)$ for small $q^2$)

- There are lots of models where PCAC is used, we are not going to discuss all of them

- There are lots of models where PCAC is used, we are not going to discuss all of them
- Usually give reasonable description of low-energy data, but not the high-energy data

# PCAC vs. black disk regime (high energy limit)

## PCAC-based models are inconsistent with BDR (even for $Q^2 = 0$):

$$\underbrace{\left.\frac{d\sigma_{\nu T\to l\pi T}}{d\nu dQ^2}\right|_{Q^2=0}}_{\text{diffractive production, } W\to\pi} = \frac{G_F^2}{2\pi} f_\pi^2 \frac{E_\nu - \nu}{E_\nu \nu} \underbrace{\sigma_{\pi T\to\pi T}}_{\text{elastic scattering}}$$

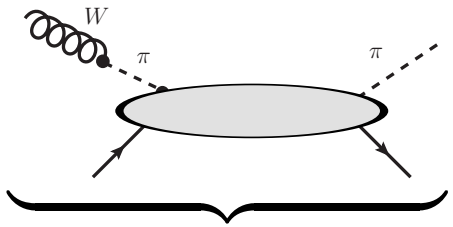


$$\sim \frac{q_\mu}{q^2 - m_\pi^2}$$

(diagrams with pions are suppressed by lepton mass, $\mathcal{O}(m_l)$)

# PCAC vs. black disk regime (high energy limit)

PCAC-based models are inconsistent with BDR (even for $Q^2 = 0$):

$$\underbrace{\left.\frac{d\sigma_{\nu T\to l\pi T}}{d\nu dQ^2}\right|_{Q^2=0}}_{\text{diffractive production, } W\to\pi} = \frac{G_F^2}{2\pi} f_\pi^2 \frac{E_\nu - \nu}{E_\nu \nu} \underbrace{\sigma_{\pi T\to\pi T}}_{\text{elastic scattering}}$$


$\sim R_A$


$\sim R_A^2$

different $A$-dependence

# PCAC vs. black disk regime (high energy limit)

PCAC-based models are inconsistent with BDR (even for $Q^2 = 0$):

$$\underbrace{\left.\frac{d\sigma_{\nu T\to l\pi T}}{d\nu dQ^2}\right|_{Q^2=0}}_{\text{diffractive production, } W\to\pi} = \frac{G_F^2}{2\pi} f_\pi^2 \frac{E_\nu - \nu}{E_\nu \nu} \underbrace{\sigma_{\pi T\to\pi T}}_{\text{elastic scattering}} F_{abs}$$


$\sim R_A$


$\sim R_A^2$

different $A$-dependence

Rein-Sehgal factor $F_{abs} \sim \exp(-const\, A^{1/3})$ does not explain the discrepancy

# Color dipole representation and neutrino-proton interactions

- Earlier have seen diagrams with gluon contribution
- In Bjorken regime ($x_B = Q^2/2m_N\nu \sim 1$) just two gluon exchange
- In the small-$x_B$ limit ($\nu \gg Q^2/2m_N$)-saturation regime

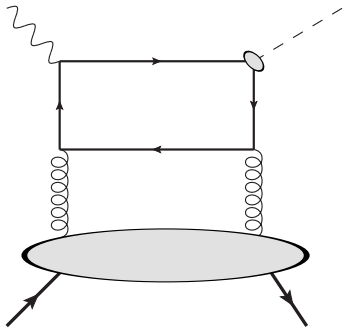

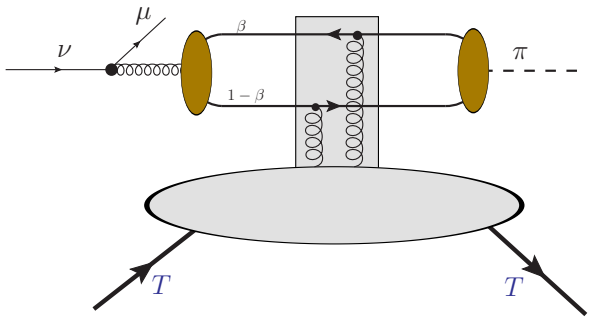


The amplitude gets a form

$$\mathscr{A}^{aT\to\pi T} = \bar{\Psi}_\pi\left(\beta',r'\right)\otimes\mathscr{A}_T^d\left(\beta',r';\beta,r\right)\otimes\Psi_a\left(\beta,r\right),$$

- $\mathscr{A}_T^d\left(\beta',r';\beta,r\right)$ universal object, depends only on the target $T$, known from $\gamma p$ and $\gamma A$ processes.
- $\bar{\Psi}_\pi, \Psi_a$ are the distribution amplitudes of the initial and final states.
  - Need to take care of chiral symmetry.
  - For study of AR and its breaking, should be valid up to $Q^2 = 0$.

For the distribution amplitude

- We use the Instanton Vacuum Model (IVM)
  - Has correct chiral properties
  - Allows systematic evaluation of the DAs to all twists
  - Gives reasonable estimate for all low-energy constants
  - For $q^2 \approx 0$ longitudinal DAs are related to pion DAs
    - ★ And this guarantees transverse structure of the amplitude in accord with $\chi$-sym:

$$T_\mu^{(a\to\pi)} = \left(\frac{q_\mu q_\nu}{q^2 - m_\pi^2} - g_{\mu\nu}\right) P_\nu \, T_{\pi\pi}(p,q) + \mathscr{O}\left(q^2\right),$$

  - $m_q$-dependence is built-in $\Rightarrow$ allows straightforward extension to $K, \eta$ without extra assumptions

# Result for the $\nu p \to \mu^- \pi^+ p$ cross-section

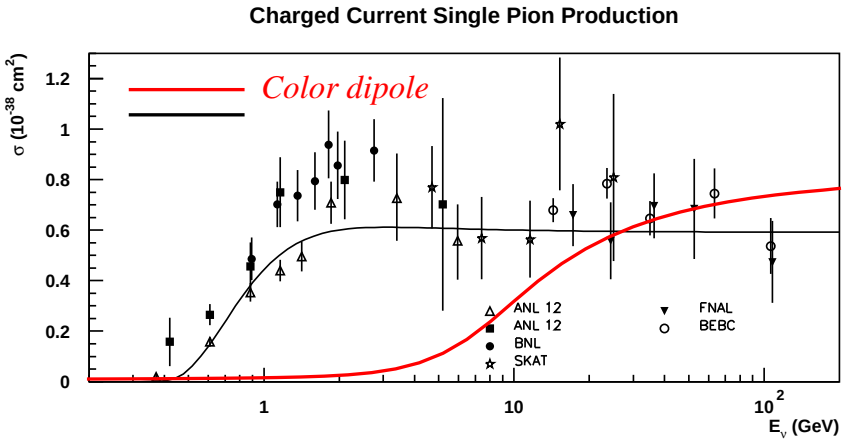


Figure: Total cross-section as a function of the neutrino energy $E_\nu$. *Compilation of experimental data from (Minerva proposal, 2004)*

- Total cross-section does not distinguish diffractive and resonance contributions
- Resonance models include a finite number of resonances, valid at low energies, constant at high energies
- At high energies $\frac{d\sigma}{dtd\ln\nu dQ^2}$ controlled by $t$-channel pomeron, $\frac{d\sigma}{dtd\ln\nu dQ^2} \sim s_{Wp}^{2\alpha} \Rightarrow \sigma_{\nu p \to l\pi p} \sim E_\nu^{2\alpha}$

# WA21 experiment @ CERN $\nu p \to \mu^- \pi^+ p$

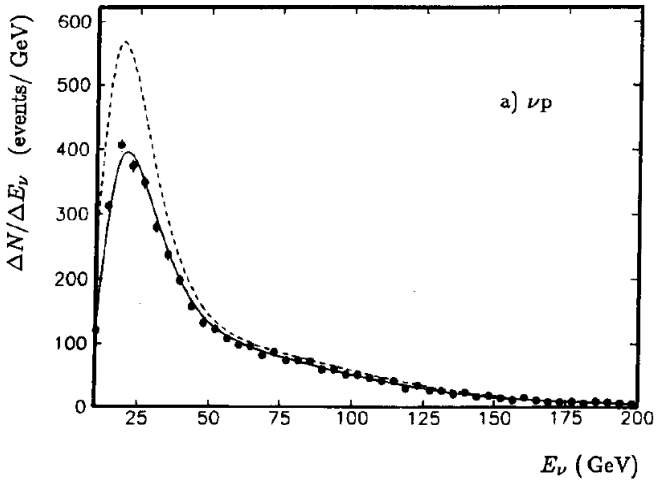


Figure: Neutrino spectrum at BEBC

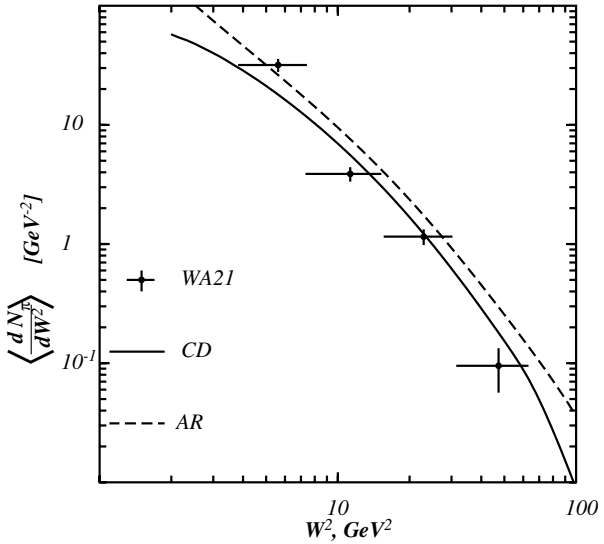


Figure: Color dipole vs. AR vs. BEBC

- Data from BEBC (CERN) (Allen et.al., 1985)
- Broad spectrum, with energies up to 200 GeV
- Due to large errorbars both color dipole and AR describe data
- No other high-energy data

# Result for the $d\sigma/dW$ cross-section

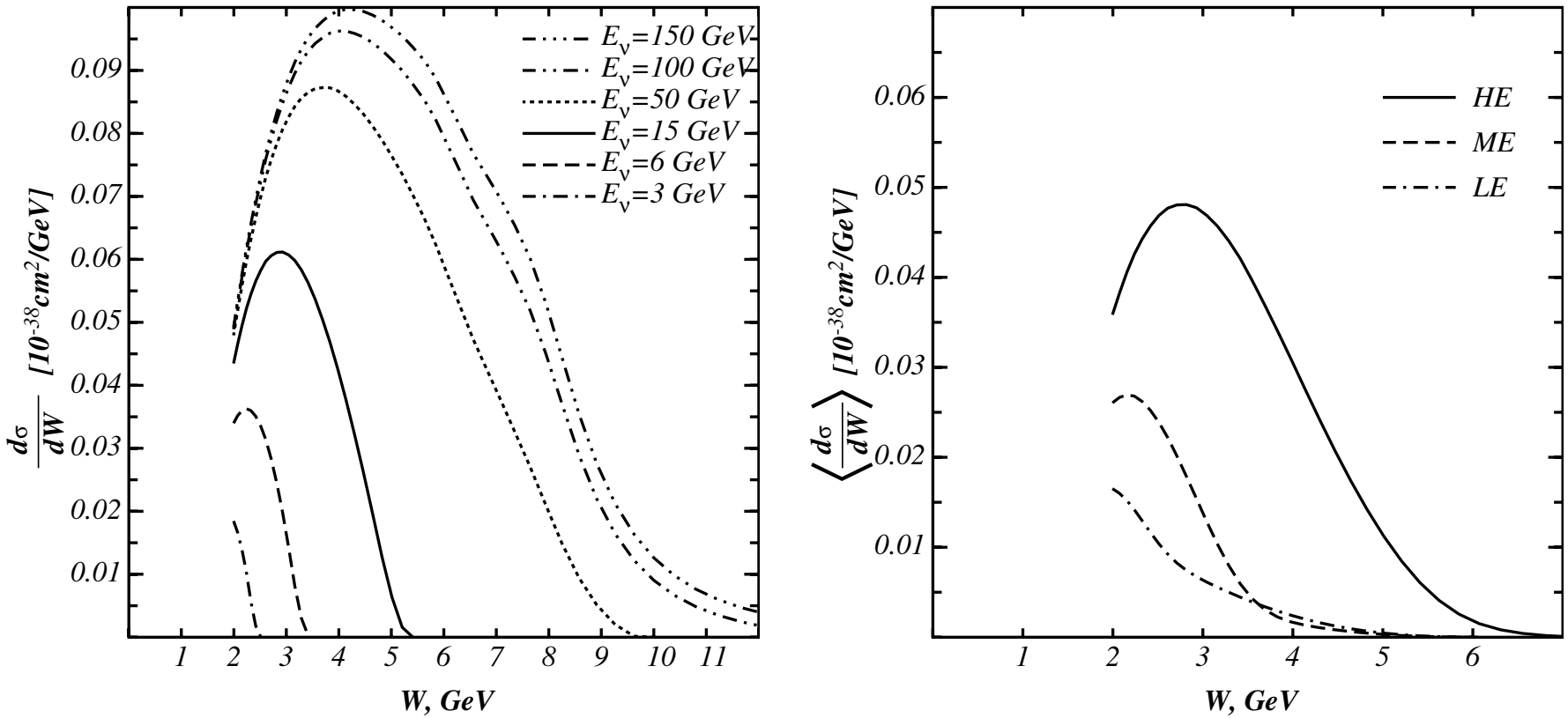


Figure: Diff. cross-section $d\sigma/dW$ and spectrum-averaged cross-section $\langle d\sigma/dW \rangle$

# Result for other mesons, $\nu d\sigma/dtd\nu dQ^2$

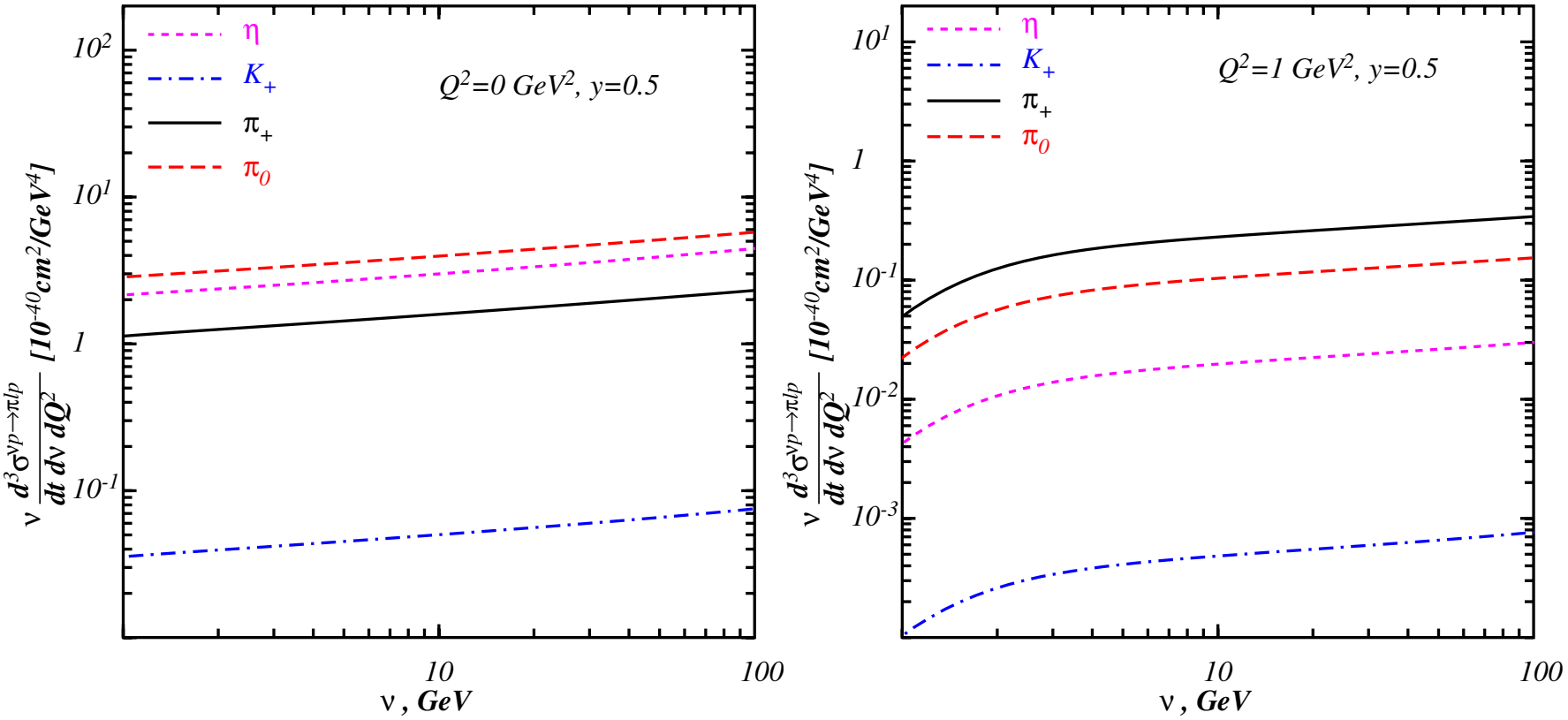


- For all mesons, $\nu$-dependence controlled by $t$-channel pomeron
- Single $K_+$-production is Cabibbo suppressed
- Single-$K_0$-production is suppressed at high energies, requires flavour exchange in $t$-channel

# Coherent neutrino-nuclear scattering

## On higher Fock states

Consider only $\bar{q}q$, contribution of $\bar{q}qg$ is suppressed for $\nu \leq 10^3$ GeV.

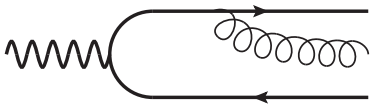

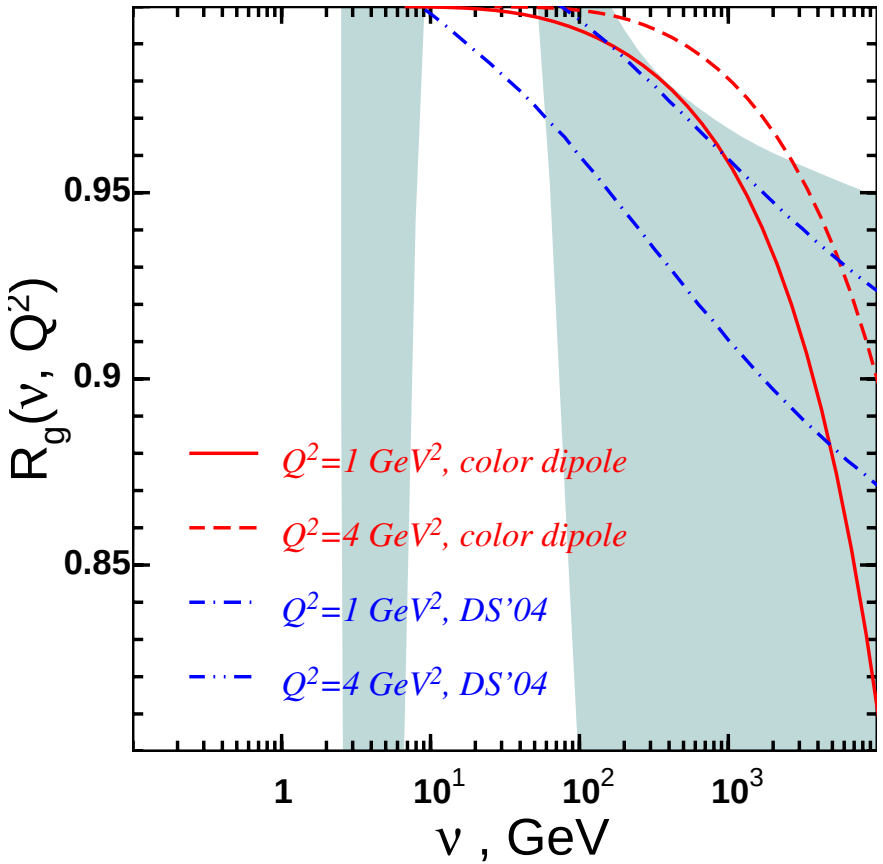


Figure: Gluon shadowing in color dipole (PRD 62, 054022 (2000)) and in phenomenological D. de Florian, R. Sassot parametrization (PRD 69, 074028 (2004)). Shaded area: gluon uncertainty band from EPS'09 parametrization (JHEP 0904:065 (2009) )

# Coherent neutrino-nuclear scattering

- Use Gribov-Glauber approach

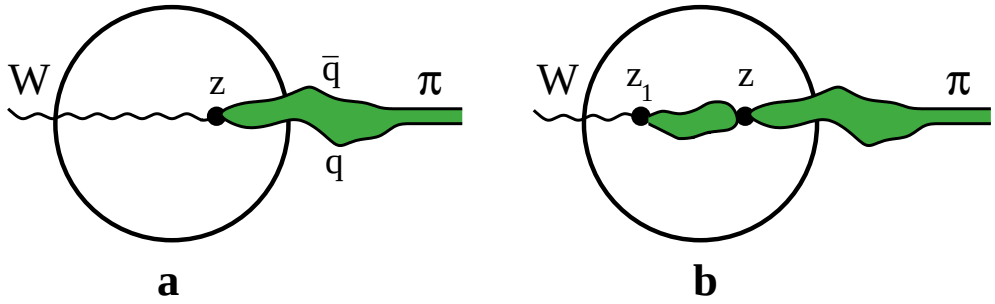


- Two scales: coherence length of the pion and effective axial meson

$$l_c^\pi = \frac{2\nu}{m_\pi^2 + Q^2}, \quad l_c^a = \frac{2\nu}{m_a^2 + Q^2}.$$

- For large $Q^2$, $l_c^\pi \approx l_c^a$ , so this case is similar to photon-nuclear processes, we have only two regimes: $l_c \gg R_A$ and $l_c \ll R_A$.
- For small $m_\pi^2 \lesssim Q^2 \ll m_a^2$, $l_c^a \ll l_c^\pi$, appears a third regime, when $l_c^a \ll R_A \ll l_c^\pi$.

# Result for the $\nu A \to l\pi^+ A$ differential cross-section (color dipole)

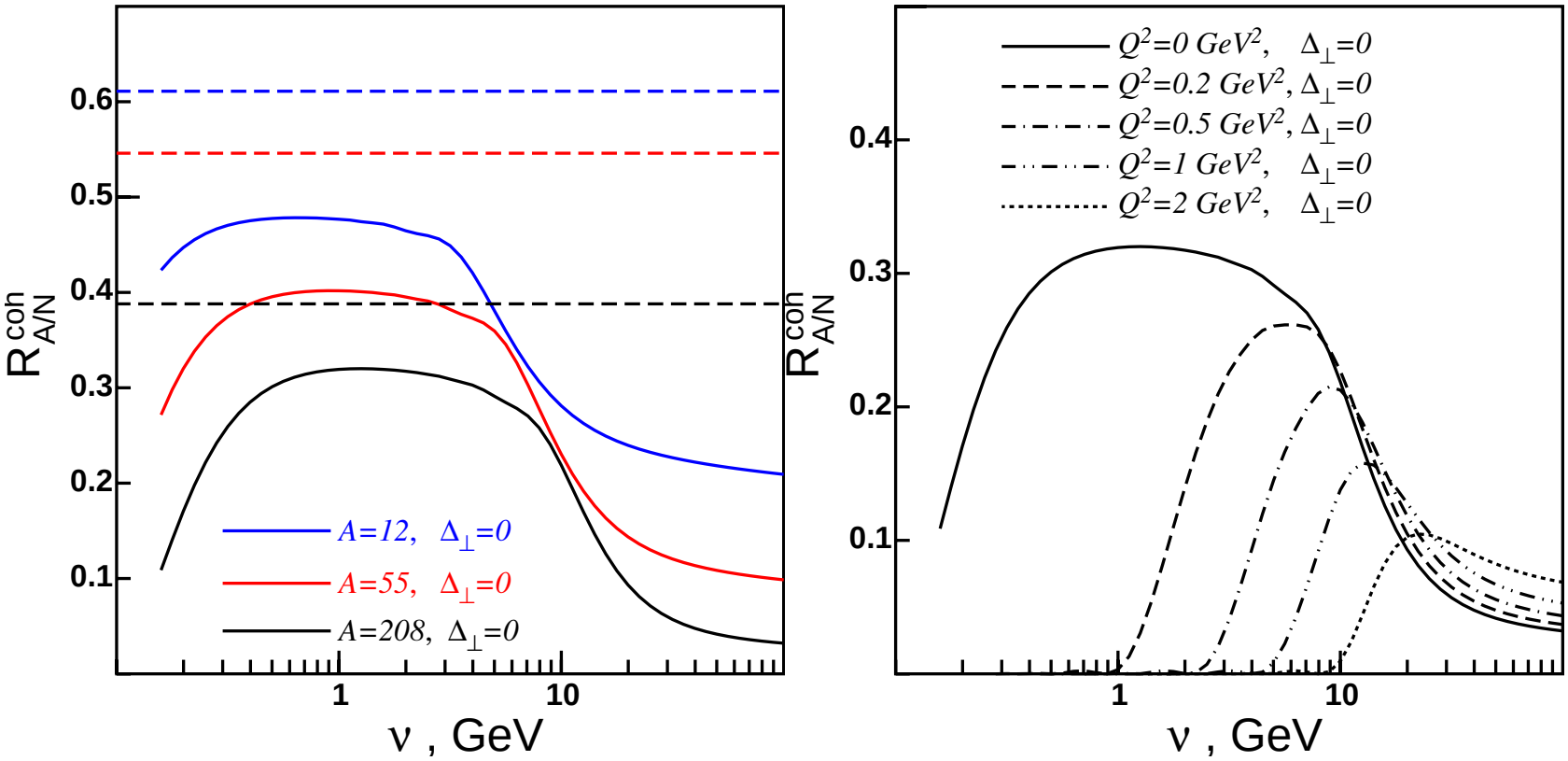


Figure: Ratio of cross-sections on the nucleus and proton.

*Adler relation on nuclei is always broken* (?!).

# $\nu A \to l\pi^+ A$ cross-section in a 2-channel model

(Phys. Rev. C84 (2011), 024608)

Cross-check in a simple *2-channel model*:

- Assume there are only pion and $a_1$ mesons
- Assume Adler relation is valid for nucleon at $Q^2 = 0$
- Use Gribov-Glauber approach for nuclei.

# Result for the $\nu A \to l\pi^+ A$ cross-section (2-channel model)

$$R^{coh}_{A/N} = \frac{1}{A}\frac{d\sigma_A/d\nu dQ^2}{d\sigma_N/d\nu dQ^2}$$

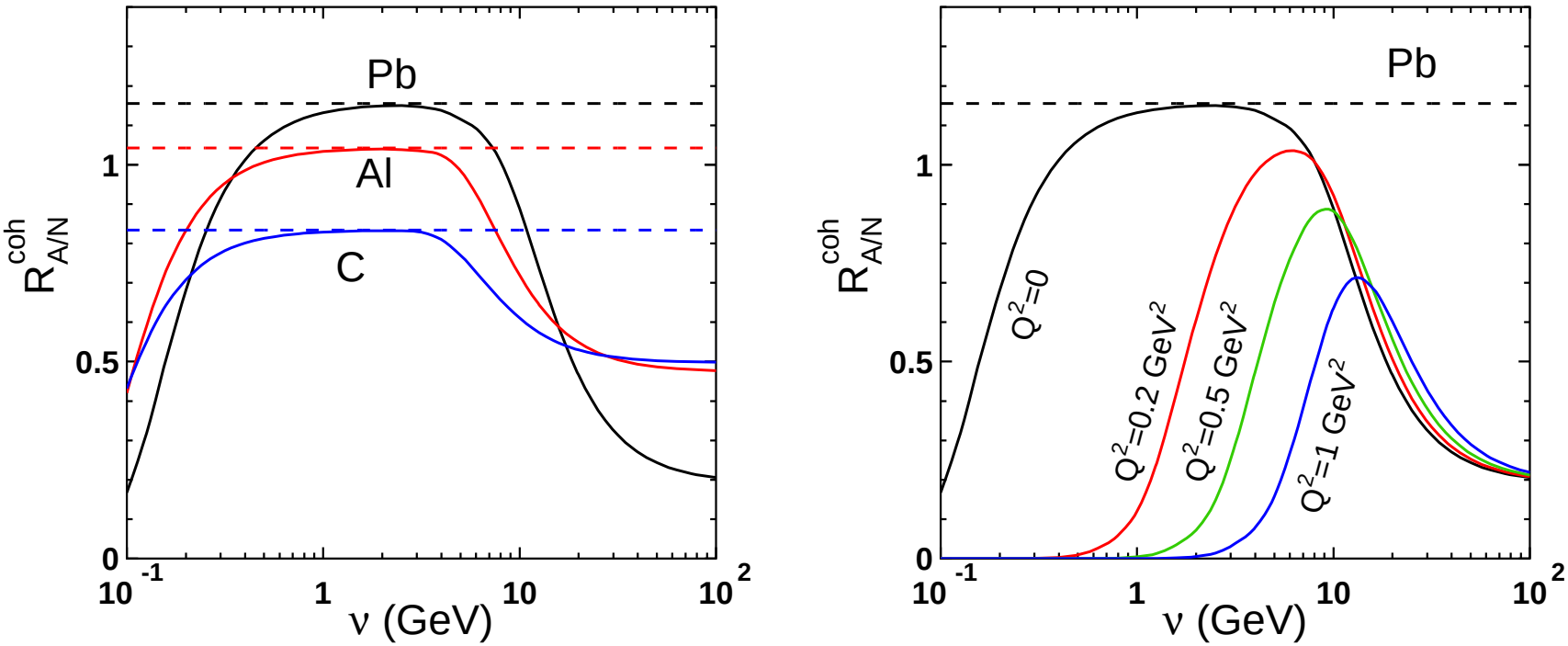


Adler relation works in the region $\nu \leq 10$ GeV; for high energies AR broken due to absorptive corrections

# $\nu A \to l\pi^+ A$ differential cross-section: CD vs. 2-channel

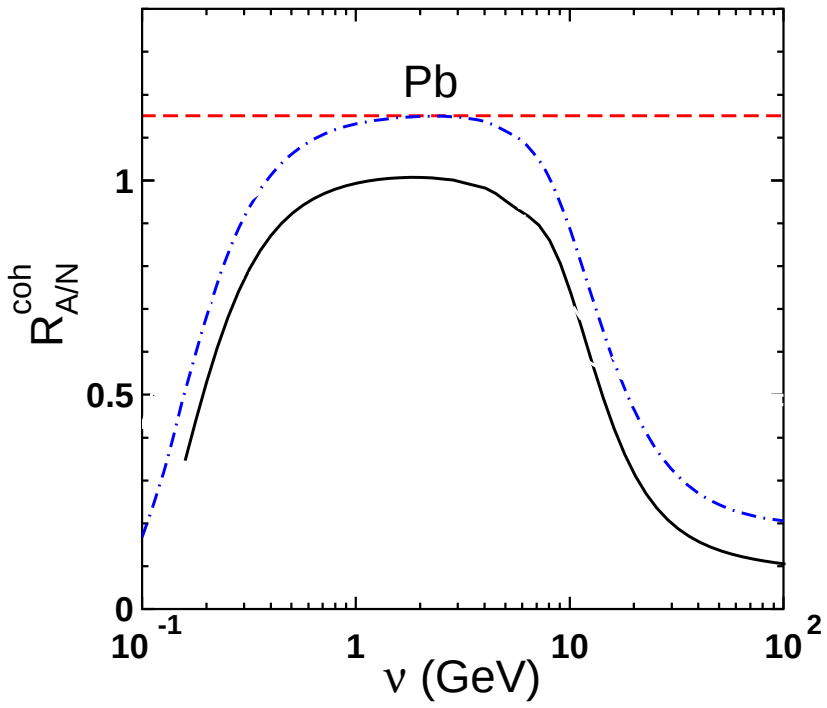


- At low energies, AR works for 2-channel model but not for color dipole.
  - Reason: axial current contains a mixture of states with different masses; for light dipoles coherence length is large.
- At higher energies, there are absorptive corrections

# High energy limit

Adler relation is broken due to absorptive corrections. Assume the limit $R_A \ll l_a \ll l_\pi$.

$$\underbrace{\left.\frac{d\sigma_{\nu T\to l\pi T}}{d\nu dQ^2}\right|_{Q^2=0}}_{\text{diffractive production, } W\to\pi} = \frac{G_F^2}{2\pi} f_\pi^2 \frac{E_\nu-\nu}{E_\nu \nu} \underbrace{\sigma_{\pi T\to\pi T}}_{\text{elastic scattering}}$$


$\sim R_A$


$\sim R_A^2$

# Result for the $\nu A \longrightarrow l\pi^+ A'$ incoherent differential cross-section

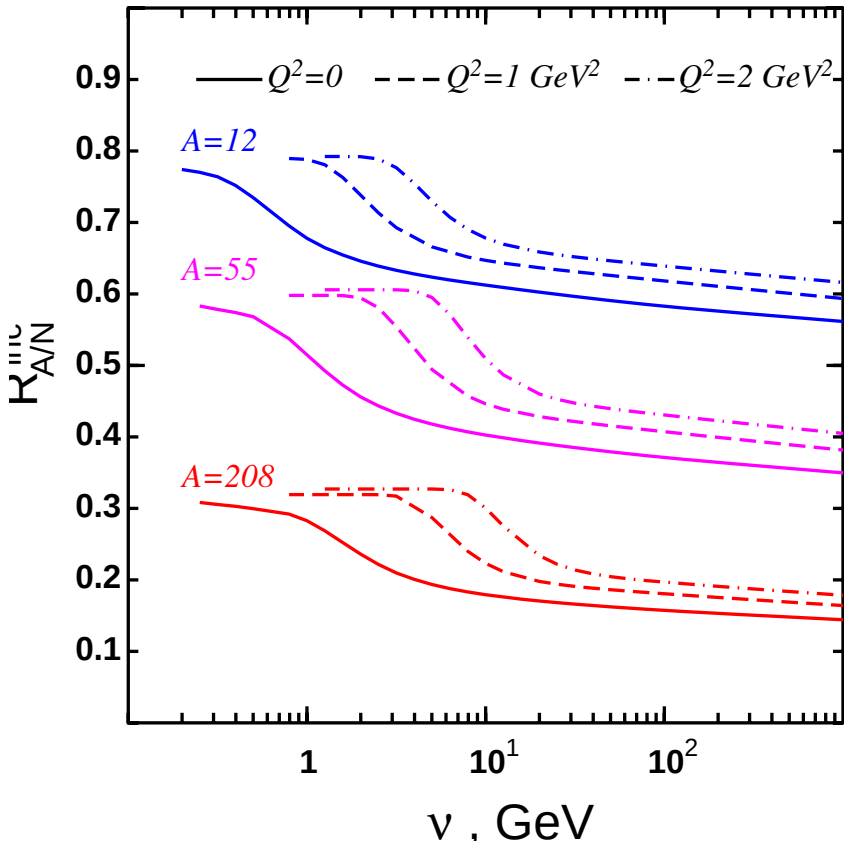


- No interference of the final pions $\Rightarrow$ Incoherent cross-section, is controlled by $l_c^a$.

# Conclusion

We discussed $\nu$-production of goldstones $(\pi, K, \eta)$ in the high-energy kinematics

- We argue that in Bjorken kinematics this process could be used to disentangle the flavour structure of the GPDs and supplement DVCS and DVMP data from $ep$
- We argue that the Adler relation is broken at high energies, and demonstrate this in the color dipole model, evaluating the goldstone production cross-section.

- Thank You for your attention !

# GPD relations to other nonperturbative objects:

Wigner distributions

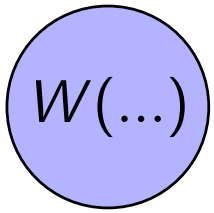


$$W(x,\xi,\vec{r},t) \sim \int dz^- e^{ixP^+z^-}$$
$$\times \left\langle P+\Delta \left| \psi^\dagger\left(-\frac{z}{2}n-\frac{\vec{r}}{2}\right)\psi\left(\frac{z}{2}n+\frac{\vec{r}}{2}\right)\right| P\right\rangle$$

- Most general object–Wigner distributions
- Partial case of Wigner distribution
- Have "siblings" – TMDs, TDAs (cross-channel)
- Contain formfactors, PDFs
- Contain lots of other info (fractions of spin, 3D-distribution, etc.)

# GPD relations to other nonperturbative objects:

Wigner distributions

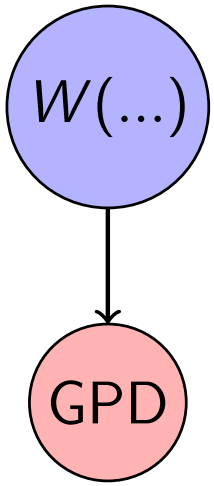


$r \to 0 \Rightarrow H(x,\xi,t)$

$$W(x,\xi,\vec{r},t) \sim \int dz^- e^{ixP^+z^-} \times \left\langle P+\Delta \left| \psi^\dagger\left(-\frac{z}{2}n-\frac{\vec{r}}{2}\right)\psi\left(\frac{z}{2}n+\frac{\vec{r}}{2}\right)\right| P\right\rangle$$

- Most general object–Wigner distributions
- Partial case of Wigner distribution
- Have "siblings" – TMDs, TDAs (cross-channel)
- Contain formfactors, PDFs
- Contain lots of other info (fractions of spin, 3D-distribution, etc.)

# GPD relations to other nonperturbative objects:

Wigner distributions

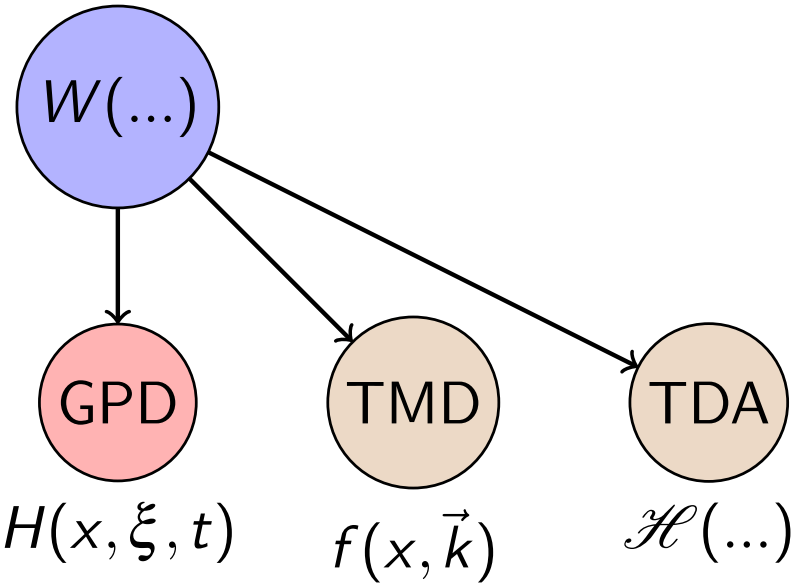


$$W(x,\xi,\vec{r},t) \sim \int dz^- e^{ixP^+z^-} \times \left\langle P+\Delta \left| \psi^\dagger \left(-\frac{z}{2}n-\frac{\vec{r}}{2}\right) \psi \left(\frac{z}{2}n+\frac{\vec{r}}{2}\right) \right| P \right\rangle$$

- Most general object–Wigner distributions
- Partial case of Wigner distribution
- Have "siblings" – TMDs, TDAs (cross-channel)
- Contain formfactors, PDFs
- Contain lots of other info (fractions of spin, 3D-distribution, etc.)

# GPD relations to other nonperturbative objects:

Wigner distributions

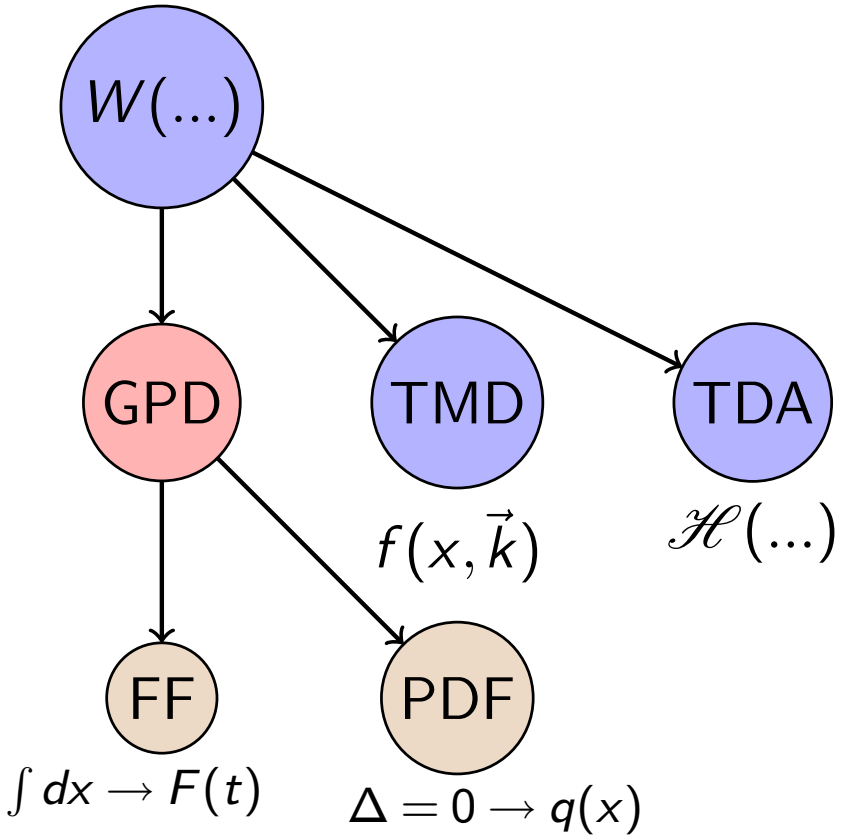


- Most general object–Wigner distributions
- Partial case of Wigner distribution
- Have "siblings" – TMDs, TDAs (cross-channel)
- Contain formfactors, PDFs
- Contain lots of other info (fractions of spin, 3D-distribution, etc.)

# GPD relations to other nonperturbative objects:

Wigner distributions

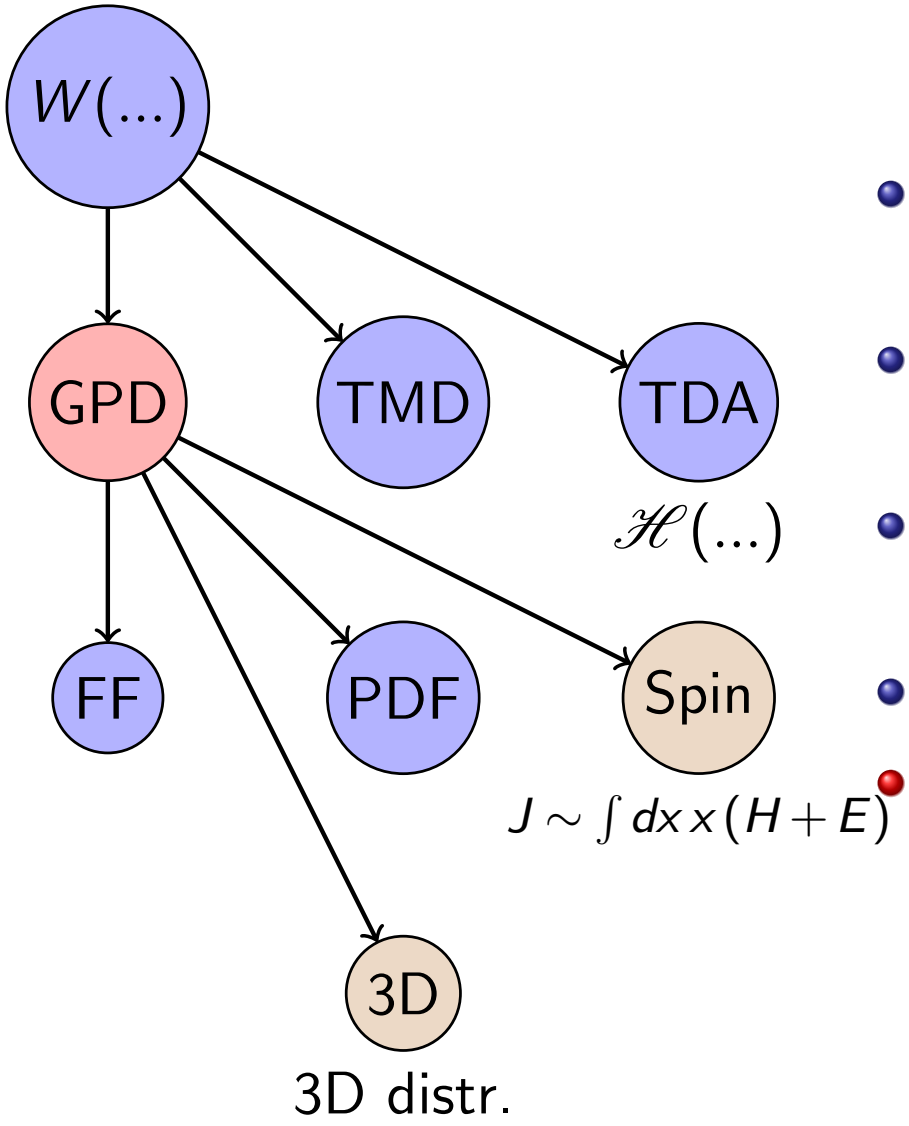


- Most general object–Wigner distributions
- Partial case of Wigner distribution
- Have "siblings" – TMDs, TDAs (cross-channel)
- Contain formfactors, PDFs
- Contain lots of other info (fractions of spin, 3D-distribution, etc.)

(Monday talk by R. McKeown)

# GPDs reference card

Currently available models fall in three classes:

- Phenomelogical approach (Radyushkin's DD, KG model etc): generate skewedness as

$$H(x,\xi,t) = \int dx' K(x,x',\xi,t) q(x')$$

  Assumed that flavour dependence comes from $q(x)$, skewedness $K(x,x',\xi,t)$ is taken the same for all flavours.

- Models based on evolution (Polyakov-Shuvaev's dual model)

$$H(x,\xi,t) = 6x(1-x)\sum_n A_n(t) C_n^{3/2}\left(\frac{x}{\xi}\right)$$

- Microscopic models

$$H(x,\xi,t) \sim \int d^3k \delta\left(k^+ - xP^+\right) \sum_n \psi_n^\dagger(k+\Delta)\psi_n(k)$$

# Current GPD uncertainties from DVCS analysis

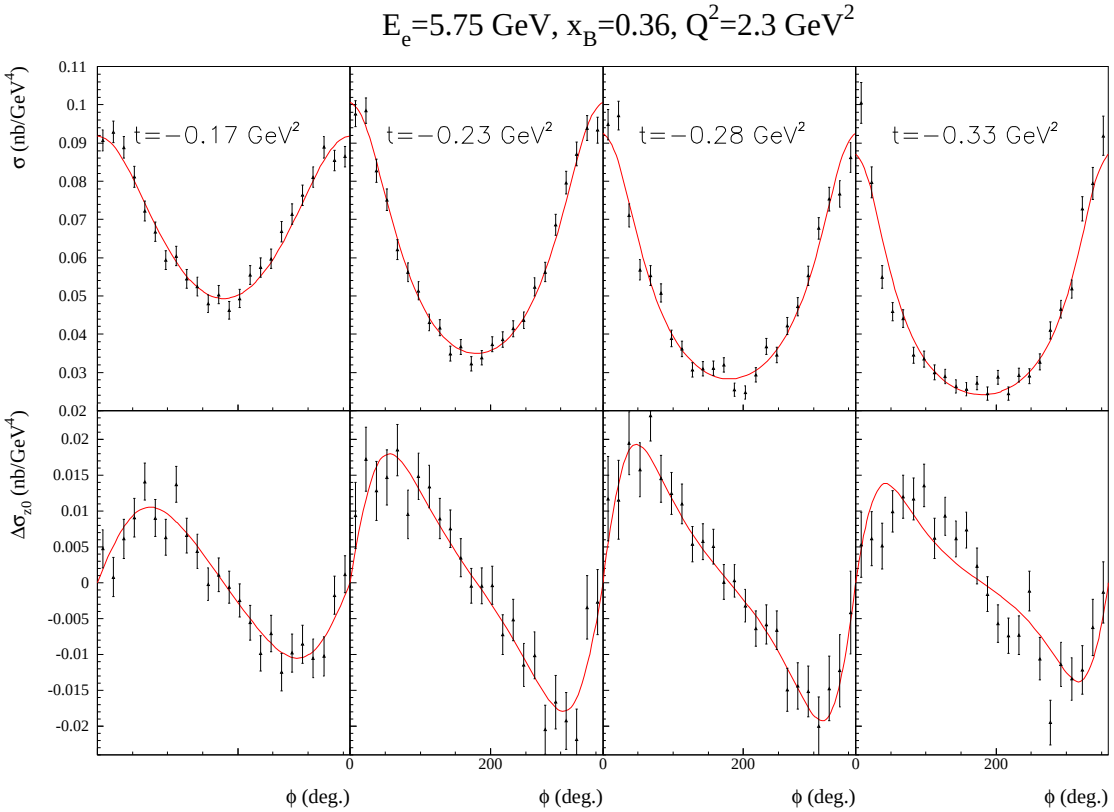


(M. Guidal, Eur.Phys.J. A37 (2008)

# Current GPD uncertainties from DVCS analysis

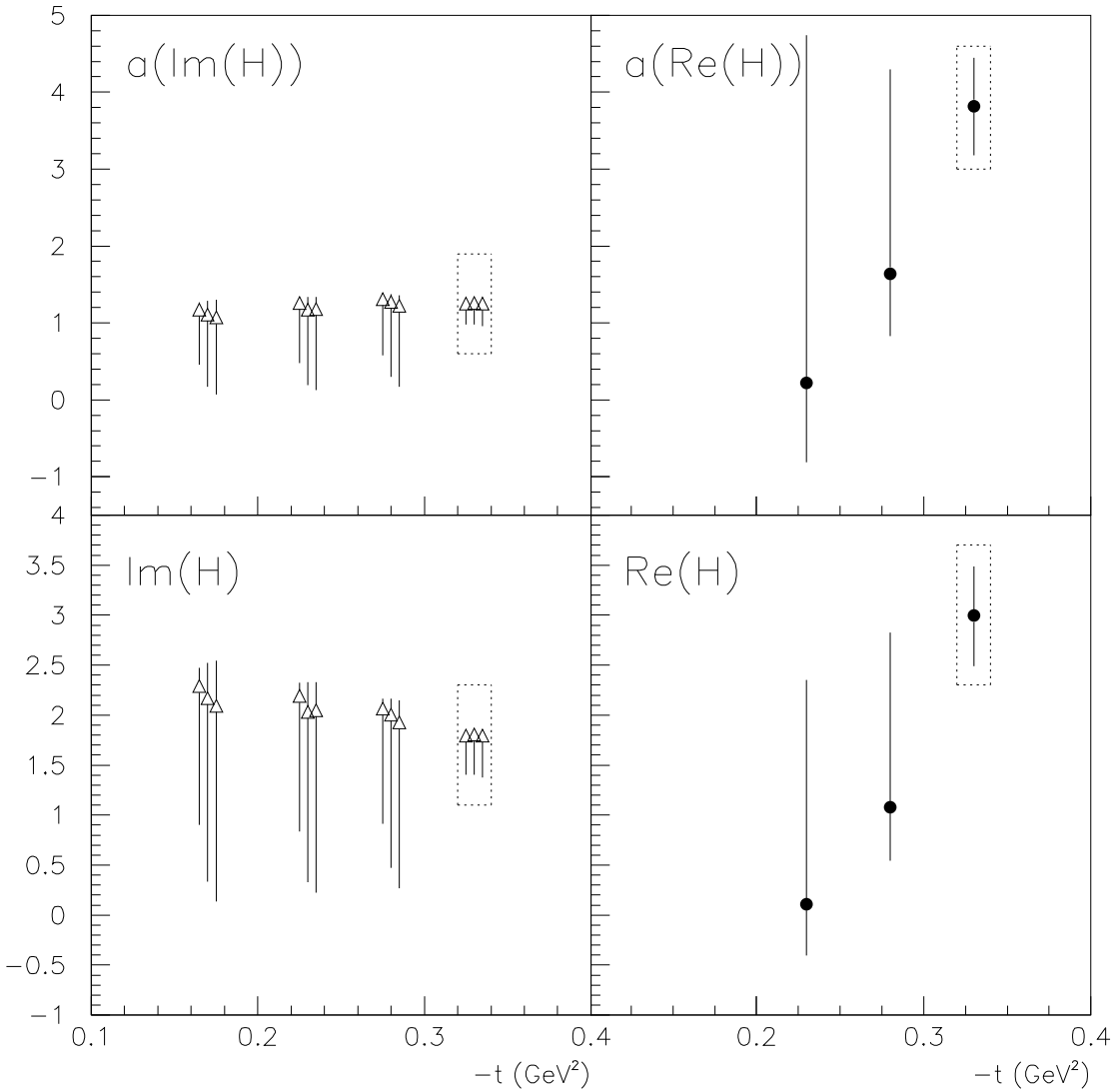


(M. Guidal, Eur.Phys.J. A37 (2008)

# Distribution amplitudes of pion

Pion distribution amplitudes (P. Ball *et al*, 2006)

$$\begin{aligned}\left\langle 0\left|\bar{\psi}(y)\gamma_\mu\gamma_5\psi(x)\right|\pi(q)\right\rangle &= if_\pi\int_0^1 du\, e^{i(up\cdot y+\bar{u}p\cdot x)}\times \\ &\times \left(p_\mu\phi_{2;\pi}(u)+\frac{1}{2}\frac{z_\mu}{(p\cdot z)}\psi_{4;\pi}(u)\right),\end{aligned}$$

$$\left\langle 0\left|\bar{\psi}(y)\gamma_5\psi(x)\right|\pi(q)\right\rangle = -if_\pi\frac{m_\pi^2}{m_u+m_d}\int_0^1 du\, e^{i(up\cdot y+\bar{u}p\cdot x)}\phi_{3;\pi}^{(p)}(u).$$

$$\begin{aligned}\left\langle 0\left|\bar{\psi}(y)\sigma_{\mu\nu}\gamma_5\psi(x)\right|\pi(q)\right\rangle &= -\frac{i}{3}f_\pi\frac{m_\pi^2}{m_u+m_d}\int_0^1 du\, e^{i(up\cdot y+\bar{u}p\cdot x)}\times \\ &\times \frac{1}{p\cdot z}\left(p_\mu z_\nu-p_\nu z_\mu\right)\phi_{3;\pi}^{(\sigma)}(u),\end{aligned}$$

# Distribution amplitude of pion

- Best known is leading twist DA $\phi_{2;\pi}(x)$

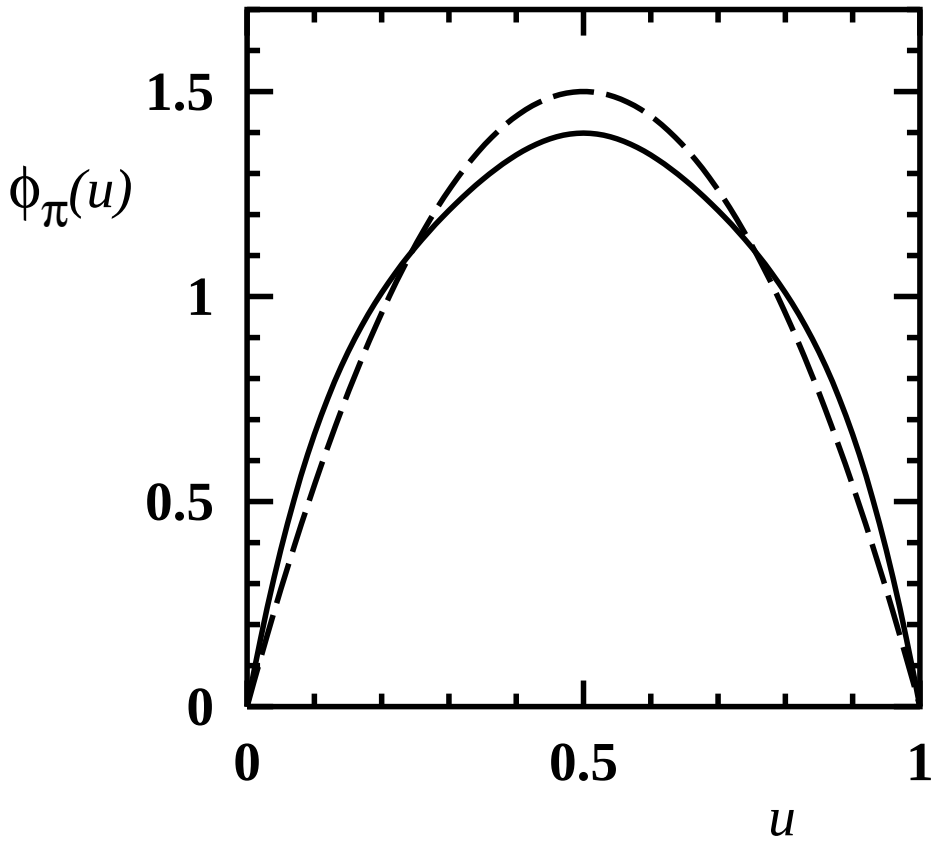


close to $\phi_{as}(x) = 6x(1-x)$ (V. Yu. Petrov *et. al.*, 1998)

- We take into account all the DAs in order not to kill the $\chi$-symmetry

# Pion DA $\phi_2(x)$ from $F_{\pi\gamma^*\gamma}$

- Common choice: $\phi_2(x) \approx \phi_{as}(z) \approx 6z(1-z)$
- $\phi(z) \sim 6z(1-z)\sum_n a_n C_n^{3/2}(2z-1)$

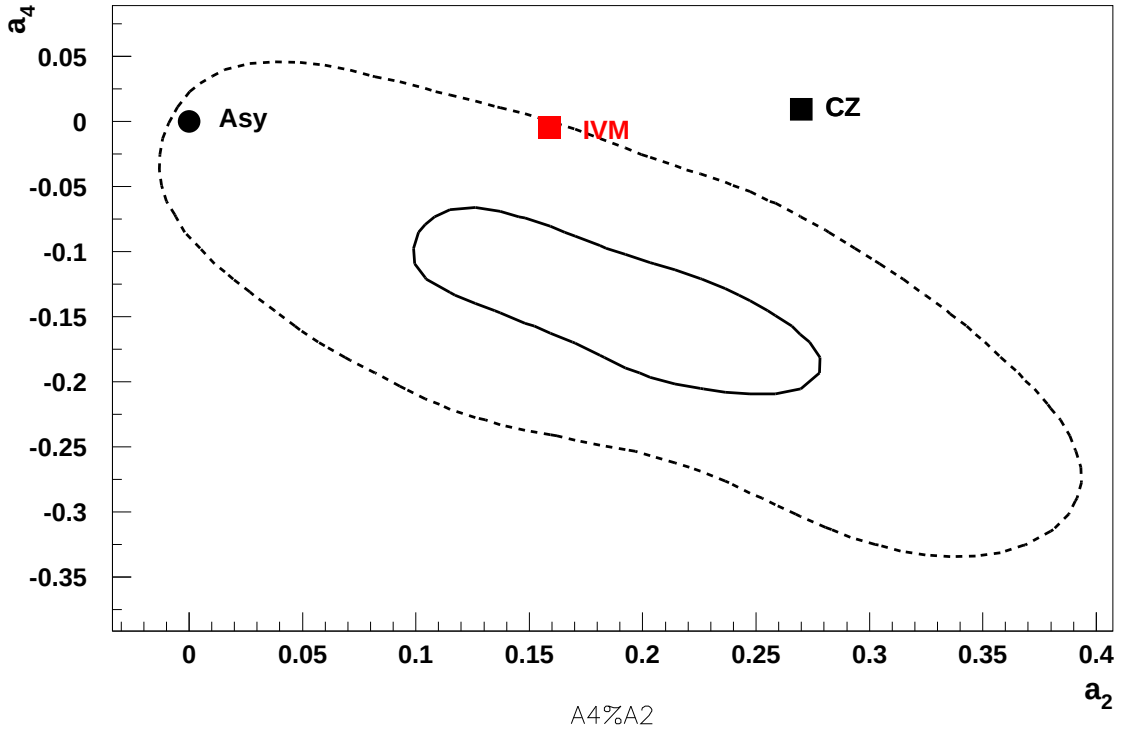


Figure: $1\sigma$ and $2\sigma$ intervals for the moments $a_2$ and $a_4$ from $F_{\pi\gamma^*\gamma}$ data (PRD 62 (2000), 116002)

# Distribution amplitudes of axial meson

## Axial DAs (K.-C. Yang 2007)

$$\langle 0|\bar{\psi}(y)\gamma_\mu\gamma_5\psi(x)|A(q)\rangle = if_A m_A \int_0^1 du\, e^{i(up\cdot y+\bar{u}p\cdot x)} \times \times \left( p_\mu \frac{e^{(\lambda)}\cdot z}{p\cdot z}\Phi_{||}(u) + e_\mu^{(\lambda=\perp)} g_\perp^{(a)}(u) - \frac{1}{2} z_\mu \frac{e^{(\lambda)}\cdot z}{(p\cdot z)^2} m_A^2 g_3(u) \right),$$

$$\langle 0|\bar{\psi}(y)\gamma_\mu\psi(x)|A(q)\rangle = -if_A m_A \varepsilon_{\mu\nu\rho\sigma} e_\nu^{(\lambda)} p_\rho z_\sigma \int_0^1 du\, e^{i(up\cdot y+\bar{u}p\cdot x)} \frac{g_\perp^{(v)}(u)}{4}$$

$$\langle 0|\bar{\psi}(y)\sigma_{\mu\nu}\gamma_5\psi(x)|A(q)\rangle = f_A^\perp \int_0^1 du\, e^{i(up\cdot y+\bar{u}p\cdot x)} \left( e_{[\mu}^{(\lambda=\perp)} p_{\nu]} \Phi_\perp(u) + \frac{e^{(\lambda)}\cdot z}{(p\cdot z)^2} m_A^2 p_{[\mu} z_{\nu]} h_{||}^{(t)}(u) + \frac{1}{2} e_{[\mu}^{(\lambda)} z_{\nu]} \frac{m_A^2}{p\cdot z} h_3(u) \right),$$

$$\langle 0|\bar{\psi}(y)\gamma_5\psi(x)|A(q)\rangle = f_A^\perp m_A^2 e^{(\lambda)}\cdot z \int_0^1 du\, e^{i(up\cdot y+\bar{u}p\cdot x)} \frac{h_{||}^{(p)}(u)}{2}.$$

# PCAC relations for DAs

PCAC relates 4 DAs of the axial current and pion DAs:

$$
\begin{aligned}
\Phi_{||}\left(\alpha, q^2 = m_\pi^2\right) &= \phi_{2;\pi}(\alpha) \\
g_3\left(\alpha, q^2 = m_\pi^2\right) &= \frac{1}{2}\psi_{4;\pi}(\alpha) \\
h_{||}^{(t)}\left(\alpha, q^2 = m_\pi^2\right) &= -\frac{1}{3}\frac{m_\pi^2}{m_u + m_d}\phi_{3;\pi}^{(\sigma)}(\alpha) \\
h_{||}^{(p)}\left(\alpha, q^2 = m_\pi^2\right) &= \frac{2m_\pi^2}{m_u + m_d}\phi_{3;\pi}^{(p)}(\alpha)
\end{aligned}
$$

# PCAC relations for DAs

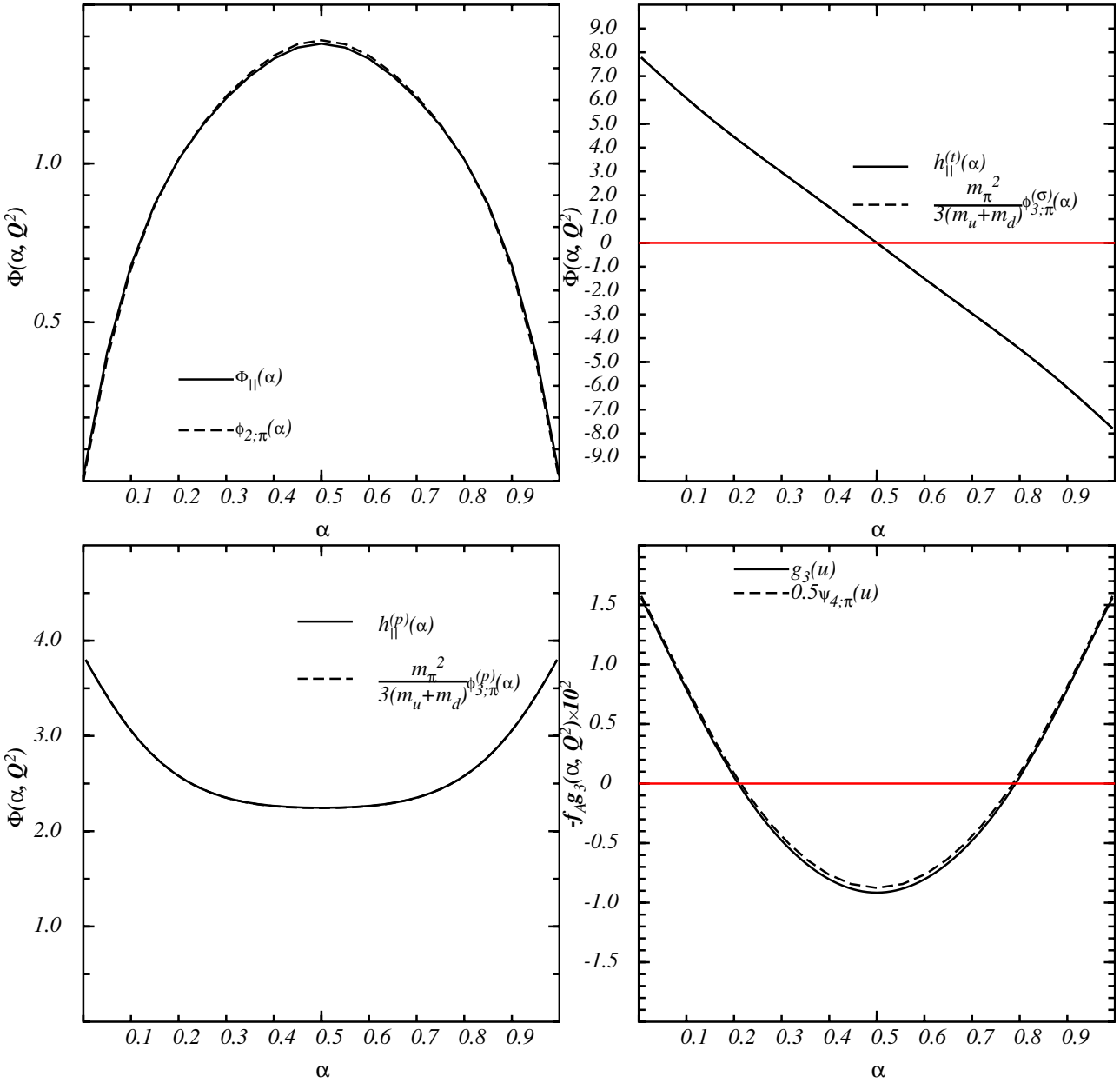

# Models

All the models used for description of the coherent $\nu \longrightarrow \pi$-production fall into three categories:

- PCAC-based models
- Low-energy microscopic models
- High-energy microscopic models

# Low-energy microscopic models

## Sufficient experimental data

(K2K [PRL 95 (2005), 252301], SciBooNE [PRD 78 (2008), 112004, PRD 81 (2010), 111102], MiniBooNE [PLB 664, 41 (2008)], ... )

In the small-$\nu$ dominant contribution comes from $s$-channel resonances

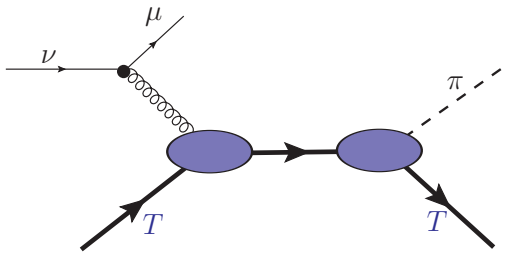


crossed diagrams give nonresonant background

- Number of resonances required increases rapidly with $s$
  - Just a few resonances which give largest contributions:
    Spin-3/2: $\Delta(1232), N(1520), \Delta(1600), \Delta(1620), ...$
    Spin-1/2: $N(1440), N(1535), N(1650), ...$

    (E. Paschos [PRD 80 (2009) 033005], O. Lalakulich, et. al. [PRD 71 (2005), 074003; PRD 74(2006), 014009], S. Nakamura, 2011;)

# Low-energy microscopic models

## Sufficient experimental data

(K2K [PRL 95 (2005), 252301], SciBooNE [PRD 78 (2008), 112004, PRD 81 (2010), 111102], MiniBooNE [PLB 664, 41 (2008)], ... )

In the small-$\nu$ dominant contribution comes from $s$-channel resonances

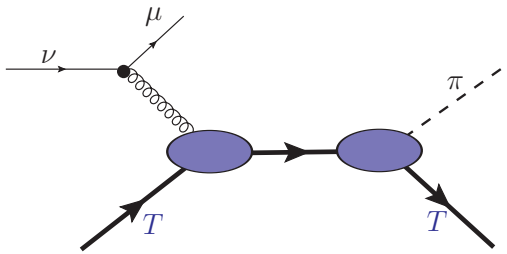


crossed diagrams give nonresonant background

- Number of resonances required increases rapidly with $s$
- Couplings are NOT local, for $\Delta(1232)$ alone there are **8** transitional formfactors

$$\langle \Delta^{++}|J^\nu|p\rangle = \sqrt{3}\bar{\psi}_\lambda(p')d^{\lambda\nu}u(p)$$

$$d^{\lambda\nu} = g^{\lambda\nu}\left[\frac{C_3^V}{m_N}\hat{q} + \frac{C_4^V}{m_N^2}(p'q) + \frac{C_5^V}{m_N^2}(pq) + C_6^V\right]\gamma_5 - q^\lambda\left[\frac{C_3^V}{m_N}\gamma^\nu + \frac{C_4^V}{m_N^2}p'^\nu + \frac{C_5^V}{m_N^2}p^\nu\right]\gamma_5$$

$$+g^{\lambda\nu}\left[\frac{C_3^A}{m_N}\hat{q} + \frac{C_4^A}{m_N^2}(p'q)\right] - q^\lambda\left[\frac{C_3^A}{m_N}\gamma^\nu + \frac{C_4^A}{m_N^2}p'^\nu\right] + g^{\lambda\nu}C_5^A + q^\lambda q^\nu\frac{C_6^A}{m_N^2}.$$

# Low-energy microscopic models

Sufficient experimental data

(K2K [PRL 95 (2005), 252301], SciBooNE [PRD 78 (2008), 112004, PRD 81 (2010), 111102], MiniBooNE [PLB 664, 41 (2008)], ... )

In the small-$\nu$ dominant contribution comes from $s$-channel resonances

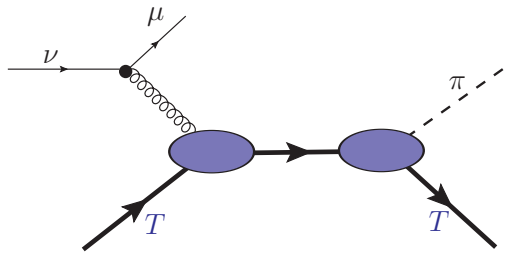


crossed diagrams give nonresonant background

- Number of resonances required increases rapidly with $s$
- Couplings are NOT local, for $\Delta(1232)$ alone there are **8** transitional formfactors
  - Completely neglect the nonlocality (Amaro et. al, PRD 79(2009),013002)
  - Parameterize everything in dipole-like form (O. Lalakulich, et. al. [PRD 71 (2005), 074003; PRD 74(2006), 014009])
    - ★ Too many formfactors, uncertainty in parameters

# Low-energy microscopic models

Sufficient experimental data

(K2K [PRL 95 (2005), 252301], SciBooNE [PRD 78 (2008), 112004, PRD 81 (2010), 111102], MiniBooNE [PLB 664, 41 (2008)], ... )

In the small-$\nu$ dominant contribution comes from $s$-channel resonances

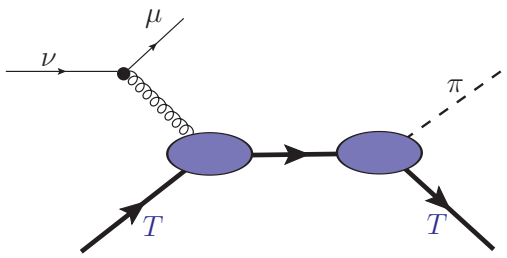


crossed diagrams give nonresonant background

- Number of resonances required increases rapidly with $s$
- Couplings are NOT local, for $\Delta(1232)$ alone there are **8** transitional formfactors
- Open questions: non-resonant background, modification of resonances inside the nuclei, ...

- High-energy microscopic model

# High-energy coh$\pi$ neutrino-production

## Limited experimental data

- The only high-statistics experiment is Minerva@Fermilab

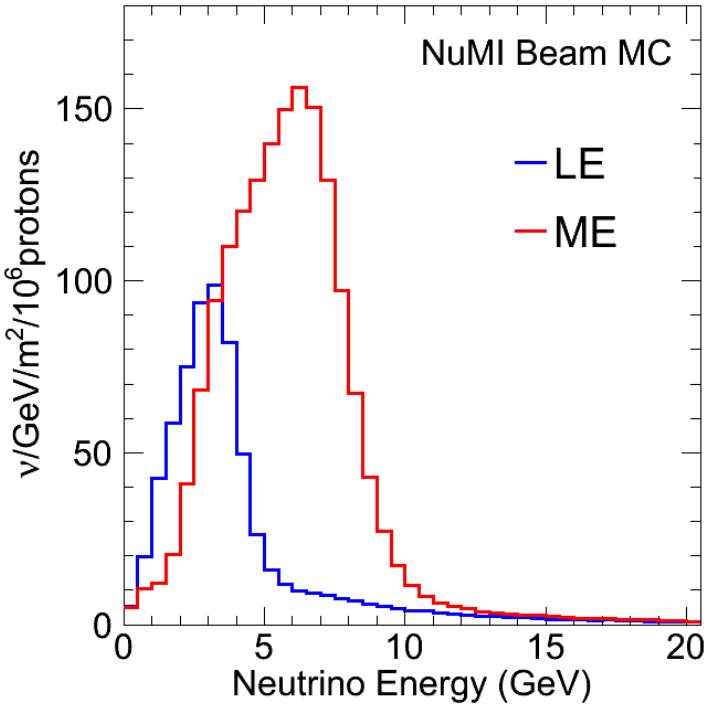


(Minerva@Fermilab, 2011)

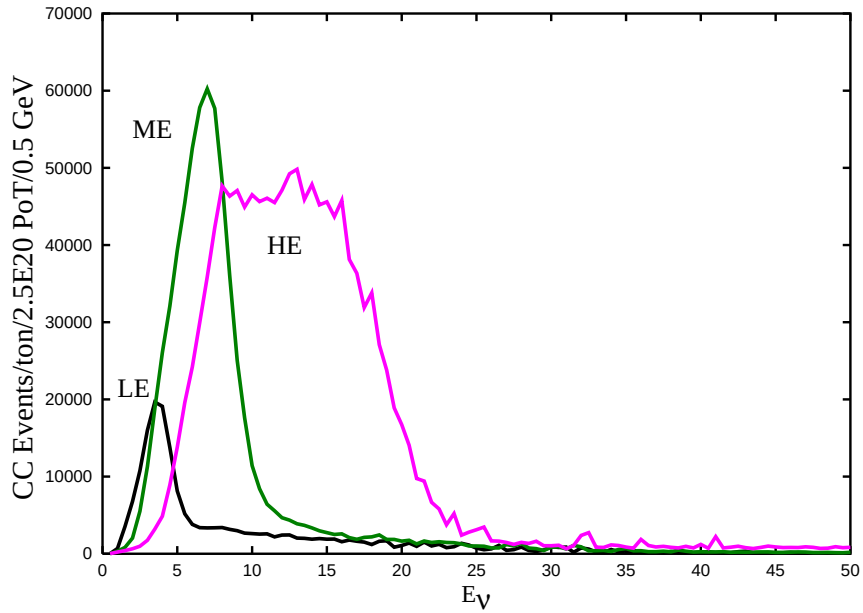


(Minerva proposal, 2004)

# High-energy coh$\pi$ neutrino-production

Limited experimental data

- The only high-statistics experiment is Minerva@Fermilab

Older experiments have poor statistics and measure total cross-sections:

- BEBC ($E_\nu \lesssim 200$ GeV) (Allen et. al. [NPB 264 (1986),221]; Marage et.al. [ZPC 31 (1986),191, ZPC 43 (1989),523])

# High-energy coh$\pi$ neutrino-production

Limited experimental data

- The only high-statistics experiment is Minerva@Fermilab

Older experiments have poor statistics and measure total cross-sections:

- BEBC ($E_\nu \lesssim 200$ GeV)
- FNAL ($E_\nu \lesssim 250$ GeV) (Aderholz et. al. [PRL 63(1989),2349]; Wilocq et.al. [PRD 47(1993),2661])

# High-energy coh$\pi$ neutrino-production

Limited experimental data

- The only high-statistics experiment is Minerva@Fermilab

Older experiments have poor statistics and measure total cross-sections:

- BEBC ($E_\nu \lesssim 200$ GeV)
- FNAL ($E_\nu \lesssim 250$ GeV)
- CHARM & CHARM-II ($E_\nu \lesssim 300$ GeV) (Bergsma et. al. [PLB 157(1985),469], Vilain et. al. [PLB 313(1993),267])

# Current GPD uncertainties from DVCS analysis

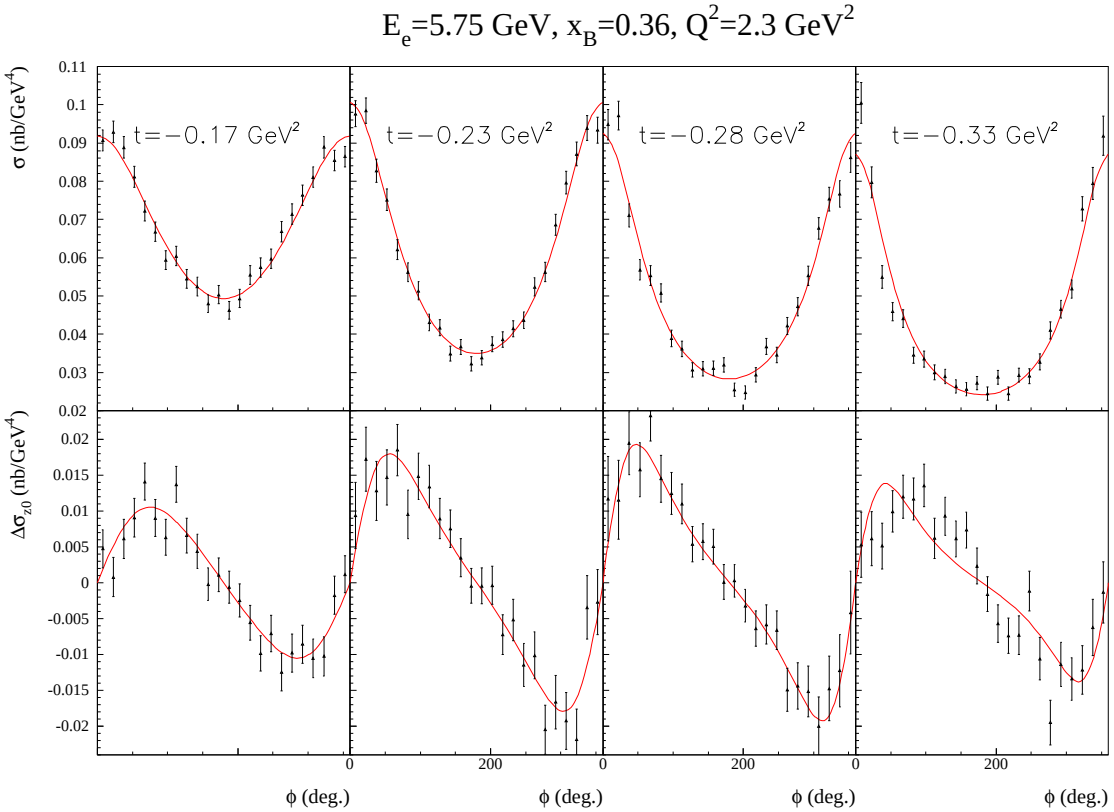


(M. Guidal, Eur.Phys.J. A37 (2008)

# Current GPD uncertainties from DVCS analysis

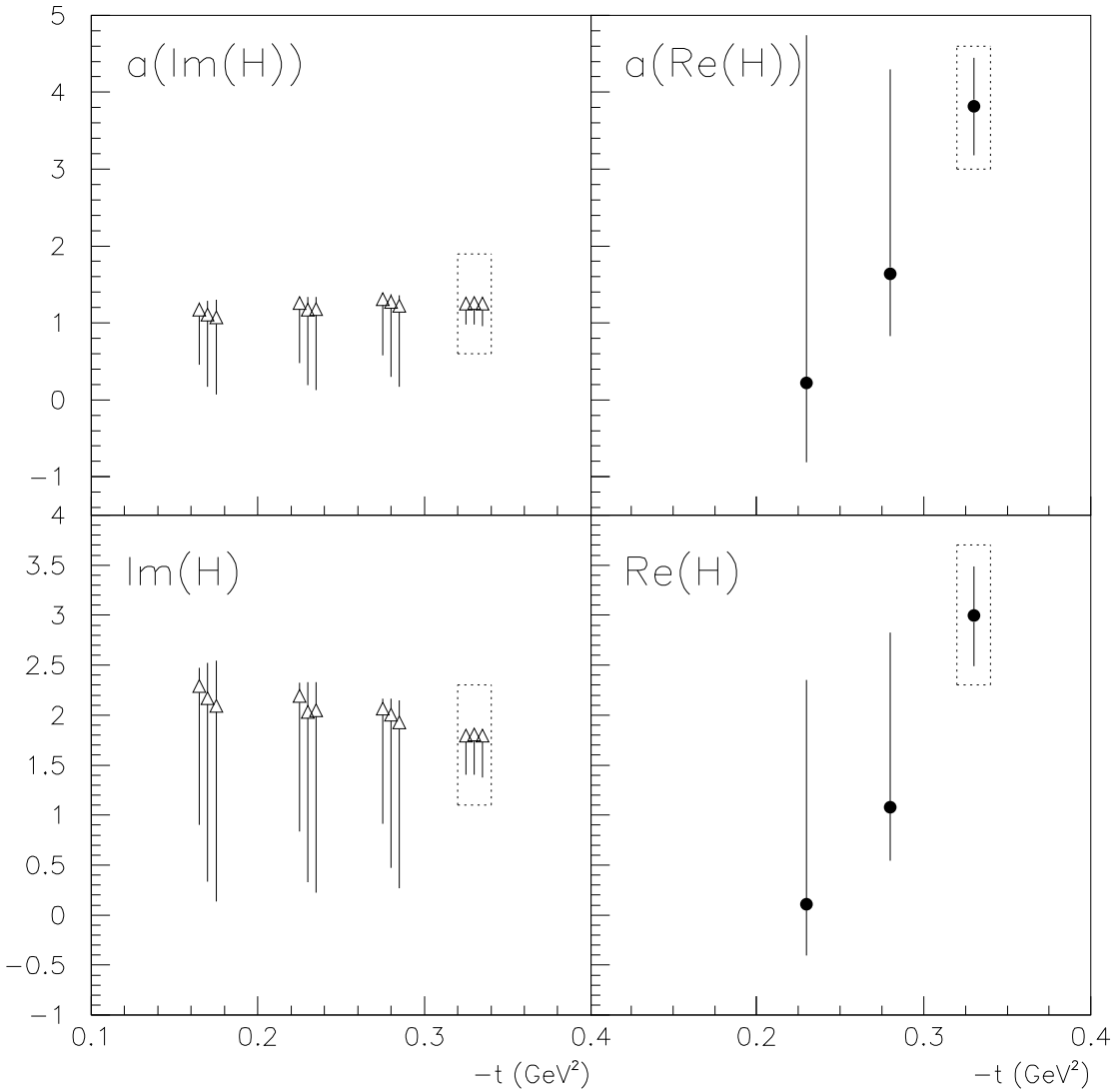


(M. Guidal, Eur.Phys.J. A37 (2008)